Isoreticular Two-Dimensional Covalent Organic Frameworks Synthesized by On-Surface Condensation of Diboronic Acids

Jürgen F. Dienstmaier,[†,‡] Dana D. Medina,[‡,§] Mirjam Dogru,[‡,§] Paul Knochel,[§] Thomas Bein,[‡,§] Wolfgang M. Heckl,[†,‡] and Markus Lackinger[†,‡,*]

[†]Deutsches Museum, Museumsinsel 1, 80538 Munich, Germany, and TUM School of Education, Technical University of Munich, Schellingstrasse 33, 80799 Munich, Germany, [‡]Center for NanoScience (CeNS), Schellingstrasse 4, 80799 Munich, Germany, and [§]Department of Chemistry, Ludwig-Maximilians-University, Butenandtstrasse 11 (E), 81377 Munich, Germany

ABSTRACT

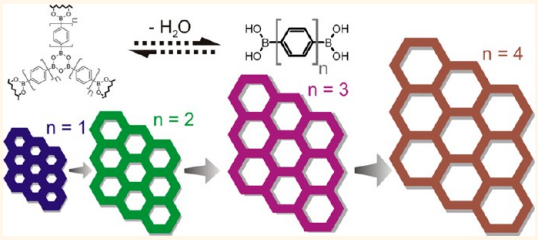

On-surface self-condensation of 1,4-benzenediboronic acid was previously shown to yield extended surface-supported, long-range-ordered two-dimensional covalent organic frameworks (2D COFs). The most important prerequisite for obtaining high structural quality is that the polycondensation (dehydration) reaction is carried out under slightly reversible reaction conditions, *i.e.*, in the presence of water. Only then can the subtle balance between kinetic and thermodynamic control of the polycondensation be favorably influenced, and defects that are unavoidable during growth can be corrected. In the present study we extend the previously developed straightforward preparation protocol to a variety of para-diboronic acid building blocks with the aim to tune lattice parameters and pore sizes of 2D COFs. Scanning tunneling microscopy is employed for structural characterization of the covalent networks and of noncovalently self-assembled structures that form on the surface prior to the thermally activated polycondensation reaction.

KEYWORDS: condensation · dehydration · scanning tunneling microscopy · surface chemistry · boronic acid · covalent organic frameworks

Two-dimensional covalent organic structures are a novel class of materials with extraordinary properties rendering them suitable for numerous potential applications in nanotechnology.[1] Especially porous networks, so-called covalent organic frameworks (COF), are of great interest for nanopatterning,[2] for organic electronics,[3,4] as nanoreactors,[5] and for immobilization of functional molecules in size-matched pores.[6] For the on-surface synthesis of covalent organic structures, different types of chemical reactions were successfully employed, most prominently radical recombination[7−15] and condensation reactions,[16−23] or a combination thereof.[24,25] In particular, the polycondensation of boronic acids on surfaces has already yielded promising results.[16,24,26,28] Moreover, both mechanisms and thermodynamics of the on-surface condensation of 1,4-benzenediboronic acid were already studied by density functional theory complemented by entropy considerations.[29] It was suggested that the surface polycondensation is endothermic and, hence, entropically driven as a result of the elimination and release of water molecules as reaction byproduct. According to Le Chatelier's principle, supplying H_2O offers a way to introduce reversibility in the condensation reaction, a key requirement for the synthesis of long-range-ordered covalent structures.[1,26,27]

Recently, we demonstrated a novel and straightforward preparation protocol for the synthesis of regular and extended surface-confined 2D COFs based on the polycondensation of 1,4-benzenediboronic acid (*cf.* **1** in Figure 1) as a model system.[27] This diboronic acid building block was also successfully used in the synthesis of COF-1 bulk crystals.[30] For the on-surface polymerization, the reaction was pursued in an open system, where an initially added amount of water and eventually the H_2O partial pressure decrease over time. On the other hand, very promising results were also accomplished by Guan *et al.* in a closed system, where H_2O was supplied by the

* Address correspondence to markus@lackinger.org.

Received for review May 29, 2012 and accepted July 9, 2012.

Published online July 09, 2012
10.1021/nn302363d

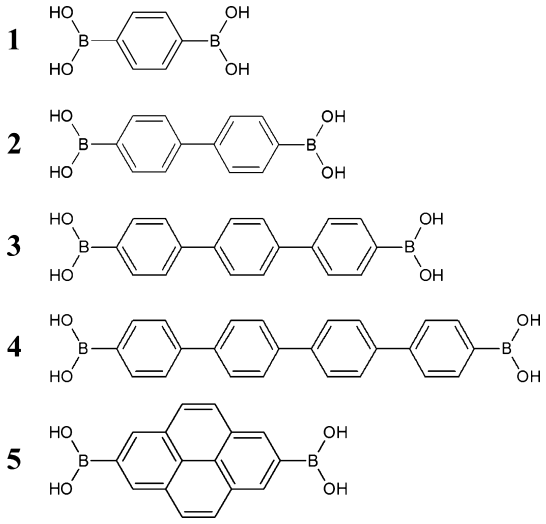

Figure 1. Molecular structures of diboronic acid monomers: 1, 1,4-benzenediboronic acid (previously studied); 2, biphenyldiboronic acid; 3, terphenyldiboronic acid; 4, quaterphenyldiboronic acid; 5, pyrene-2,7-diboronic acid.

temperature-dependent and reversible dehydration of $CuSO_4 \cdot 5H_2O$.[26] In both sets of experiments graphite (001) served as an inert substrate and is not believed to play a vital chemical role in the polymerization. For 2D COF synthesis according to the first method, **1** was dissolved in an organic solvent (alkanes, aliphatic alcohols, or carboxylic acids) and drop-cast onto the substrate. The polymerization was initiated by a thermal treatment in an open system. The final structure is formed when the water has vanished and covalent interlinks are no longer reversible. The 2D COFs were characterized by scanning tunneling microscopy (STM), and the covalent cross-linking was unambiguously verified by comparison of experimental with theoretical lattice parameters, aided by verification of both the monolayers' high thermal stability and the accompanying chemical changes by X-ray photoelectron spectroscopy.[27] The above straightforward synthesis protocol yields full surface coverage with 2D COF-1 featuring domain sizes exceeding 40 × 40 nm^2.

While in the previous work the proof of principle was demonstrated, we now extend our studies to show that the proposed synthesis protocol can also yield structurally diverse 2D COFs with increased pore dimensions. Adjustable pore sizes are an important prerequisite to specifically design host systems for variably sized guests as large functional molecules.[31] To this end, we adapt a well-established synthesis strategy of isoreticular organic structures, where the length of an organic spacer group of the monomer is increased by adding conformationally rigid entities as phenyl or ethinyl groups, while maintaining the steric arrangement of linker groups. Yaghi *et al.* and Dichtel *et al.* successfully implemented this principle with para-diboronic acids for bulk COFs.[30,32,33] Since the linear arrangement of the two boronic acid functionalities is

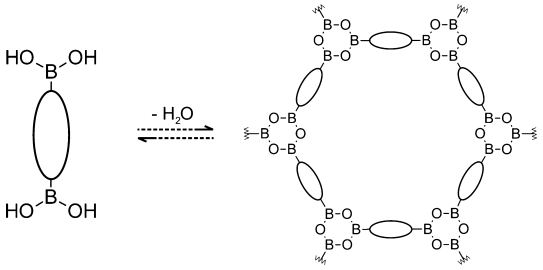

Figure 2. General reaction scheme of diboronic acid self-condensation into hexagonal 2D COFs. The straight organic backbones of the diboronic acids are symbolically represented by ellipses.

maintained, the network topology is not changed. In addition, we demonstrate that not only *p*-polyphenyl diboronic acids but also a para-diboronic acid with an aromatic pyrene backbone are suitable monomers for 2D COFs. While the same pyrene diboronic acid already yielded bulk COFs with a layered structure,[34] the synthesis of a single surface-supported 2D COF layer represents a major step toward templated growth.

Since boronic acids are known to form stable hydrogen-bonded structures, we now also study noncovalent self-assembly of the building blocks at the liquid−solid interface. This is important, because hydrogen-bonded complexes of boronic acids were identified as significant intermediate structures in the self-condensation reaction.[29] Consequently, self-assembled diboronic acid monolayers may be an important precursor structure for the polycondensation and might also influence 2D COF formation in the subsequent thermal treatment. Self-assembled structures of **1** were already observed upon deposition onto silver and gold surfaces under ultrahigh-vacuum (UHV) conditions.[35,36] Although the basic experimental conditions between UHV and the liquid−solid interface are fundamentally different and the interaction between monomers and metals is typically stronger, preceding supramolecular phases may play a general role in polymerization reactions of monomers that can also form relatively stable hydrogen-bonded structures.

RESULTS AND DISCUSSION

The cyclic self-condensation of three boronic acids yields planar boroxine rings (B_3O_3), whereby three H_2O molecules per boroxine ring are eliminated.[26,30,34] Accordingly, self-condensation of diboronic acids can result in fully reticulated planar networks, as has been demonstrated for both 2D and layered 3D systems. The self-condensation of diboronic acids yields covalent sheets with a hexagonal arrangement of boroxine rings that are interconnected by the organic backbone of the diboronic acid monomer. The general reaction scheme of the self-condensation is outlined in Figure 2. Here the polycondensation reaction is carried out in an open system. Reversible reaction conditions are realized by adding a small amount of water to the bottom

TABLE 1. Summarized Experimental and Molecular Mechanics (MM)-Derived Lattice Parameters for All 2D COFs and MM-Derived Adsorption Energies on Graphite for All Diboronic Acid Building Blocks

	experimental lattice parameters			MM-derived lattice parameters				
building block	*a* [nm]	*b* [nm]	γ [deg]	*a* [nm]	*b* [nm]	γ [deg]	pore size[b] [nm]	MM adsorption energy [kJ/mol]
1[a]	1.4 ± 0.1	1.4 ± 0.1	60.0 ± 3	1.5	1.5	60	1.0	254.6
2	2.1 ± 0.3	2.1 ± 0.3	58.9 ± 4	2.3	2.3	60	1.6	405.4
3	2.9 ± 0.2	2.9 ± 0.2	57.5 ± 3	3.0	3.0	60	2.4	535.8
4	3.5 ± 0.3	3.6 ± 0.3	62.0 ± 5	3.8	3.8	60	3.2	685.1
5	2.1 ± 0.1	2.1 ± 0.1	58.9 ± 2	2.3	2.3	60	1.4	511.3

[a] Derived in a previous study.[27] [b] Maximum diameter of a disk that fits into a pore in a van der Waals representation of the respective 2D COF.

of the reactor, and the polymerization is initiated by tempering to ~100 °C. During the heating procedure the water evaporates and the chemical equilibrium is eventually fully shifted to the dehydrated state. Details of the protocol can be found in the Materials and Methods section.

Chemical modification of the organic backbone is the strategy pursued to increase the pore size of COFs with the aim to establish an isoreticular series of 2D COFs. This general design principle for organic materials is well known from supramolecular monolayers,[37,38] isoreticular metal organic frameworks (MOF),[39] and 2D metal coordinated networks[40] and has also been exploited successfully for bulk crystals of various diboronic acid-derived COFs.[30,34,41,42] The compounds utilized in this study are illustrated in Figure 1: benzene diboronic acid (**1**) as used in the previous study, biphenyldiboronic acid (**2**), terphenyldiboronic acid (**3**), quaterphenyldiboronic acid (**4**), and pyrene-2,7-diboronic acid (**5**). The organic backbones of all diboronic acids are composed of phenyl rings, either σ-bonded (**1**−**4**) or fused into a pyrene core (**5**). Planar adsorption of these organic backbones is driven by $\pi-\pi$ interactions with the graphite substrate, whereby the adsorption energies increase with backbone size. The two boronic acid functional groups are attached in para-position, hence providing straight linkers. Assuming a fully planar geometry of the polyphenyl backbone as known from adsorbed polyphenyls,[40,43] all building blocks have D_{2h} symmetry. In order to obtain crystallographic reference data for all 2D COFs, their theoretical lattice parameters were calculated by molecular mechanics (MM) calculations; results are listed in Table 1 and compared to experimental data. Additionally, the MM-derived adsorption energies with respect to the gas phase are provided.

Utilizing the standard synthesis procedure, all building blocks yielded well-ordered 2D COFs on graphite; representative STM images of all networks are depicted in Figure 3. In the following the results obtained for the not previously studied diboronic acids (**2**−**5**) are described in more detail.

Biphenyldiboronic Acid (2). Self-condensation of **2** yields 2D COFs with a domain size of up to 100 × 100 nm^2 and

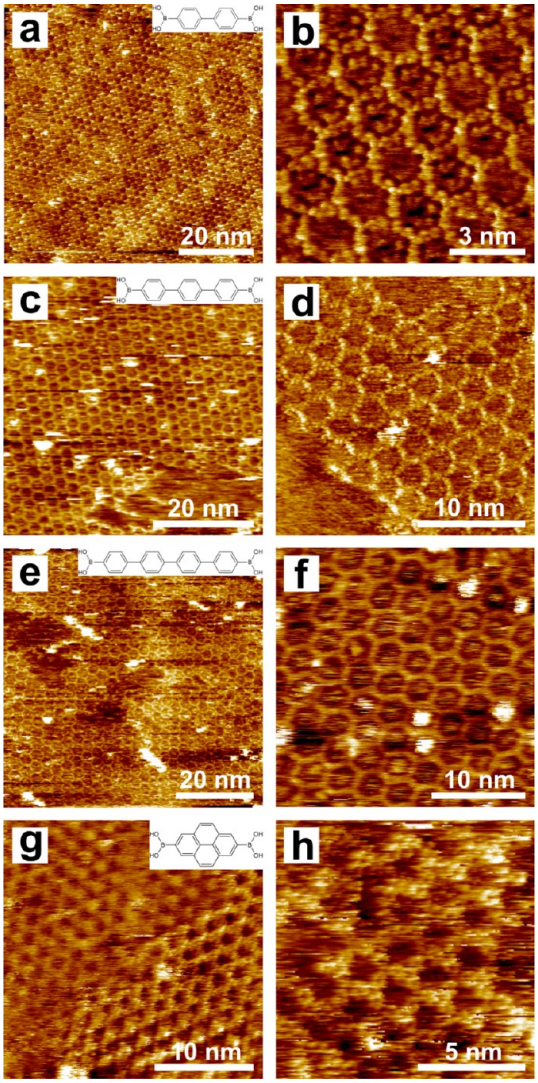

Figure 3. STM images of 2D COFs derived from polycondensation of the following monomers: (a, b) 2, (c, d) 3, (e, f) 4, (g, h) 5. The respective monomers are depicted in the insets. Details for all 2D COFs can be found in the text.

almost full surface coverage, as illustrated in Figure 3a and b. In the detailed view, contrast features within the pores are clearly discernible and are attributed to either residual solvent molecules or unreacted monomers. The experimental lattice parameter of this *p6mm*

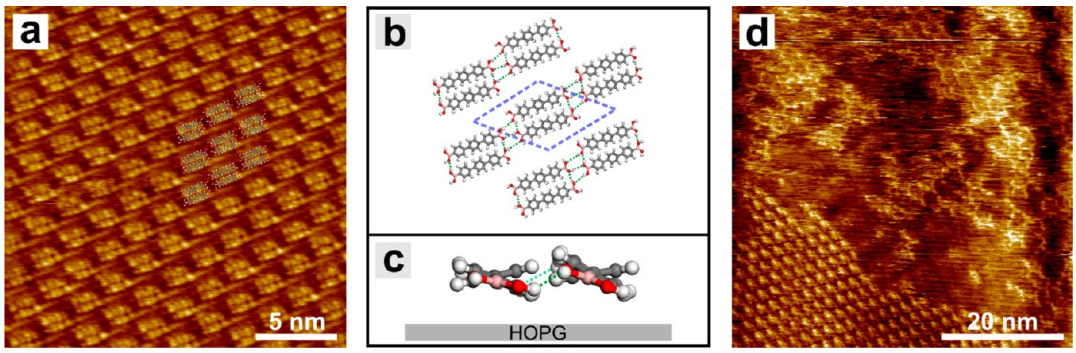

Figure 4. (a) STM image of self-assembled monolayers of terphenyldiboronic acid (3) acquired at the liquid−solid interface with heptanoic acid. Overlaid molecules are drawn to scale. (b) Tentative model as derived from the STM data. Unit cell and hydrogen bonds are indicated by dashed blue and green lines, respectively. (c) Side-view of the model with tilted molecular planes with respect to the substrate. Such tilting is suggested by the small inter-row spacing and was similarly found in comparable bulk crystals and monolayers of 1. (d) STM image of a thermally treated sample (70 °C, 30 min) showing the coexistence of unreacted self-assembled domains (lower left part) and first 2D COFs (upper right part).

symmetric structure of 2.1 ± 0.3 nm agrees well with the theoretical value of 2.3 nm and thereby confirms covalent interlinking into the anticipated network structure. In a recent study, the diboronic acid **2** was likewise polymerized in a closed system, where the hexagonal networks had similar lattice parameters.[26] Noncovalent self-assembly of **2** into stable structures could not be observed at the heptanoic acid−graphite interface at room temperature. However, a gentle thermal treatment at temperatures that are significantly lower than the 100 to 150 °C previously used to activate the polymerization on graphite[26,27] already promotes self-condensation.

Samples were thermally treated at 50 °C for ∼30 min (without reactor) and studied *ex situ* after they had cooled to room temperature. Subsequent STM imaging revealed small to intermediate domains of the 2D COF. This indicates that with monomer **2** the reaction can already be initiated at around 50 °C on graphite and that the presence of additional water is not required for the initial growth of small domains. However, without addition of water full surface coverage was never accomplished.

Terphenyldiboronic Acid (3). Domains of a 2D COF with lateral extensions up to 100 × 100 nm^2 are routinely obtained through polycondensation of **3** by applying a thermal treatment similar to that for **2** with similar temperatures and exposure times. Almost full surface coverage with only a few voids or missing molecules was achieved, and representative STM images are depicted in Figure 3c and d. Again, the experimental lattice parameter of this *p6mm* symmetric 2D COF of 2.9 ± 0.2 nm agrees well with the MM-derived lattice parameter of 3.0 nm.

Noncovalent Self-Assembly of 3. In contrast to **1** and **2** (diboronic acids with only one or two phenyl rings) the terphenyl diboronic acid **3** was also found to self-assemble into interfacial monolayers that are stabilized by noncovalent interactions. These supramolecular structures were studied on samples without any previous thermal treatment directly at the heptanoic acid−graphite interface with the STM tip immersed into solution. As evident from the STM images presented in Figure 4a, the supramolecular monolayers almost fully cover the surface. The structure possesses an almost hexagonal lattice with a = 2.1 ± 0.1 nm, b = 2.2 ± 0.1 nm, and γ = 62 ± 3°. Single molecules are clearly identified by both their size and shape as well as by their intramolecular contrast with three clearly separated protrusions. These can be assigned to the three individual phenyl rings of the terphenyl backbone.[44] The unit cell contains two molecules; a tentative model of the structure is shown in Figure 4b. As deduced from the molecular arrangement, the structure is stabilized by five B−O···H−O hydrogen bonds per unit cell. The model suggests that molecules may not adsorb entirely planar, but slightly tilted, as illustrated in Figure 4c. This tilt aids in reducing the steric hindrance of the otherwise too tightly packed polyphenyl backbones of adjacent molecules and, thus, promotes a higher surface packing density. Similar tilting was proposed for **1** both in the sheets of bulk crystals[45] and in self-assembled 2D structures on a KCl surface.[46] Interestingly, a comparable thermal treatment to that for **2** at a similar temperature of 50 °C but up to ∼1 h was not sufficient to initialize polymerization of **3**. Instead, the self-assembled monolayer persisted. 2D COFs start to nucleate only upon exposure to higher temperatures, around 70 °C, for ∼30 min. However, as illustrated in Figure 4d, covalent domains still coexist with self-assembled structures. Again, by means of a simple thermal treatment without H_2O, full surface coverage of a 2D COF was never accomplished.

A solvent dependence was observed for thermal treatment at 120 °C in the reactor with additional water. Using heptanoic acid as solvent, only COFs were observed, but no self-assembled structures anymore. Yet after a similar thermal treatment with dodecane as solvent, COFs and self-assembled supramolecular structures still coexisted. This solvent effect can be

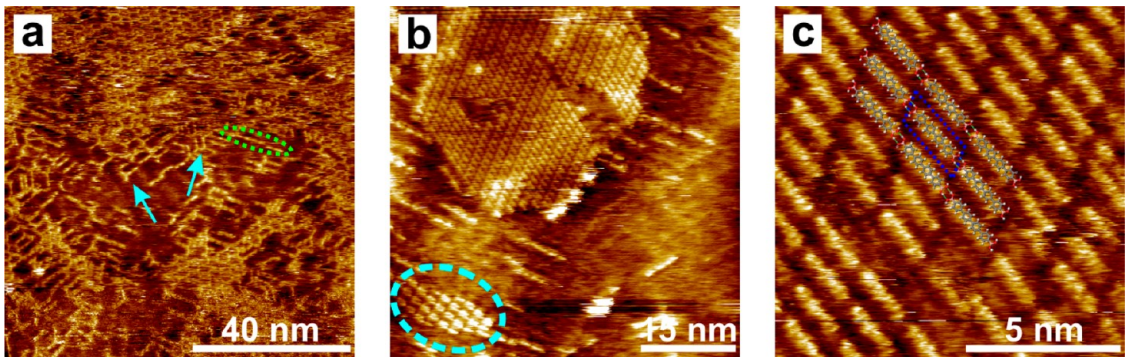

Figure 5. STM images depicting self-assembled and covalently interlinked structures of quaterphenyl diboronic acid (4). (a) Example of incomplete polymerization, where hexagonal covalent networks and remainders of the self-assembled structures coexist. The light blue arrows point to tripod structures where single boroxine rings were already formed by condensation of three monomers. The linear arrangements, marked by the dotted oval, are residues of the self-assembled structure. (b) Self-assembled structures of a nontreated sample; two different polymorphs are commonly observed: structure 1 with one molecule per unit cell and lattice parameters $a = 1.1 \pm 0.1$ nm; $b = 2.1 \pm 0.1$ nm; $\gamma = 62 \pm 3°$ (marked by the dashed circle); structure 2 with two molecules per unit cell and $a = 2.0 \pm 0.1$ nm; $b = 2.3 \pm 0.1$ nm; $\gamma = 53 \pm 2°$ (upper part). (c) Close-up of structure 1 with overlaid scaled molecules. The unit cell is marked in blue.

rationalized by the different nature of both solvents: Heptanoic acid is a polar, protic solvent, whereas dodecane is a nonpolar, nonprotic solvent. Since the molecular packing density in the self-assembled monolayer is around 1.4 times higher than in the porous COF, desorption is a necessary preceding step for COF formation. At the liquid–solid interface, the desorption barrier from the surface into the liquid phase depends on the ability of the solvent to accommodate the adsorbate. Since boronic acids can be significantly better dissolved in heptanoic acid where the molecules can be stabilized by hydrogen bonds, a lower desorption barrier promotes COF formation in heptanoic acid. Albeit less obvious, desorption of the monomers into a supernatant liquid phase might also play a key role in the experiments of Guan *et al.*,[26] where in a closed system water pressure is built up by the reversible dehydration of $CuSO_4 \cdot 5H_2O$. The authors state that full dehydration would result in a H_2O partial pressure of 8 atm. Although the actual water pressure might be lower, it appears likely that at sizable H_2O partial pressures a thin water film can form even on hydrophobic graphite surfaces. This liquid layer would promote desorption of the water-soluble diboronic acids. Consequently, a comparable reaction mechanism becomes conceivable for both preparation protocols.

Quaterphenyldiboronic Acid (4). Applying the same synthesis protocol with compound **4** yields 2D COFs with domains up to 40 × 40 nm^2, and representative STM images are depicted in Figure 3e and f. Again, a good agreement between the experimental lattice parameter of this hexagonal structure of 3.5 ± 0.3 nm with the MM-derived value of 3.8 nm proves formation of the anticipated covalent network. As shown in Figure 3e and f, despite the structural perfection and the long-range order of the networks, only partial surface coverage was accomplished. Additional changes in the preparation protocol including higher oven temperatures for the thermal treatment (140 °C instead of 120 °C) or iterations of the synthesis protocol on the same sample, where new solution was added to a pre-existing COF and further thermal treatment was applied, did not improve the surface coverage.

Often molecular arrangements at different stages of the polymerization process, *i.e.*, self-assembled structures, larger covalent aggregates, and emerging COF structures, were found to coexist on the surface; an example is shown in Figure 5a.

Noncovalent Self-Assembly of 4. Likewise noncovalent self-assembly of **4** was studied at the liquid–solid interface by the method described above. However, well-ordered self-assembled monolayers were not observed upon room-temperature deposition, but rather disordered adsorption of single molecules. Only if the samples were heated at 50 °C for ~1 h (without reactor, residues of solvent still present) were two different well-ordered, noncovalent self-assembled polymorphs observed *ex situ* after the sample had cooled. The first, more often observed structure depicted in Figure 5b exhibits lattice parameters of $a = 1.1 \pm 0.1$ nm, $b = 2.1 \pm 0.1$ nm, and $\gamma = 61 \pm 3°$ with one molecule per unit cell. The second structure is highlighted by the circle in Figure 5b and features two molecules per unit cell with lattice parameters $a = 2.0 \pm 0.1$ nm, $b = 2.3 \pm 0.1$ nm, and $\gamma = 53 \pm 2°$. Here the arrangement in the monolayer is similar to the self-assembled structure found for **3** (cf. Figure 4a). Interestingly, for the quaterphenyldiboronic acid, even a thermal treatment at 70 °C did not initiate the polymerization. Only thermal treatment at temperatures around 100 °C in the reactor eventually yielded COFs.

Pyrene-2,7-diboronic Acid (5). While in the previous examples we have demonstrated the possibility to extend lattice parameters and pore sizes by

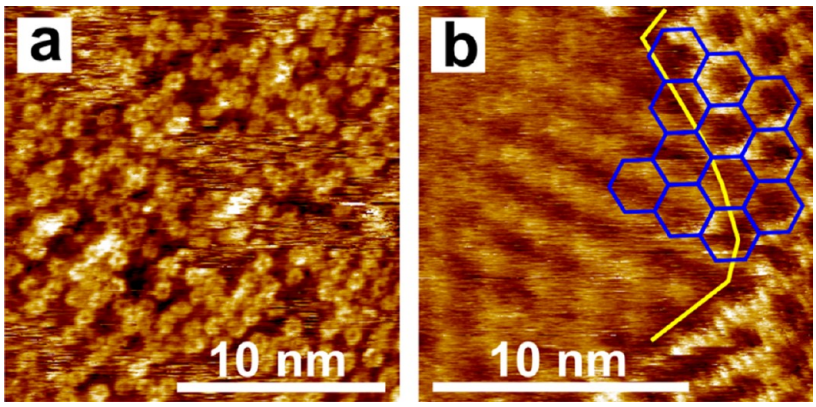

Figure 6. STM images of pyrene-2,7-diboronic acid (5) on graphite. (a) Disordered noncovalent arrangement observed at the liquid−solid interface upon room-temperature deposition of heptanoic acid solution. (b) Related 2D COF, obtained after thermal treatment of 5. At the right-hand side a second layer of the 2D COF can be discerned by the brighter contrast. First and second layer are stacked in an eclipsed manner, as indicated by the blue hexagons.

progressively adding phenyl rings to the organic backbone of diboronic acids, we now demonstrate that the nature of the organic backbone can likewise be modified. To this end we have chosen pyrene-2,7-diboronic acid, because corresponding bulk COFs have shown interesting optoelectronic properties.[34] By shining light on electrically contacted COFs in a gap configuration, photocurrents could be measured. The bulk structure obtained from solvothermal self-condensation of **5** exhibits a layered structure with eclipsed stacking of the covalent sheets.

For the synthesis of 2D COFs the same preparation protocol can be applied to **5** and yields 2D COFs with domains up to 100 × 100 nm^2 in size, as shown in Figure 3g and h. The structural quality of these COFs is high, and the defect density is very low. As for the polyphenyl networks, formation of the desired covalent network is again proven by the good agreement between the experimental (2.1 ± 0.1 nm) and theoretical lattice parameter of 2.3 nm. Both values are consistent with the in-plane lattice parameter of 2.22 nm of the corresponding bulk structure.[34]

Self-assembly of well-ordered noncovalent structures of **5** was never obtained, not even for thermally treated samples. However, short-range-ordered arrangements of **5** were observed at the heptanoic acid−graphite interface; a typical STM image is depicted in Figure 6a. These disordered arrangements persisted, even when the samples were heated at 70 °C for ∼1 h.

DISCUSSION

All diboronic acids studied were suitable building blocks for the synthesis of long-range-ordered 2D COFs on graphite. The lattice parameters of all COFs agree well with theoretical values from MM calculations and available experimental data, whereby formation of covalent networks through the anticipated cyclocondensation is verified.

An exceptional case is the pyrene-derived COF, where formation of a second layer is often observed; representative STM images are depicted in Figures 3g and 6b. Formation of bilayer COFs was found in particular for higher concentrations of the monomer **5** in the applied solution. High-resolution images with only partial coverage of the second layer allow to directly deduce the relative arrangement between both covalent layers in real space. This is demonstrated in Figure 6b by superimposing the common hexagonal lattice. The pyrene-derived COF exhibits eclipsed stacking, as similarly proposed for the corresponding bulk COF structure.[34]

For a better understanding of the underlying reaction mechanism, it is instructive to also study noncovalent self-assembly of the respective diboronic acids. Interestingly, self-assembled structures of the diboronic acids at the liquid−solid interface were observed only for the intermediately sized diboronic acids **3**, **4**, and **5**. Intermolecular hydrogen bonds that are mediated by the free boronic acid groups add to the stabilization of those monolayers. The absence of self-assembled monolayers of the smaller boronic acids **1** and **2** can be explained by their relatively low adsorption energies, which are apparently too small to stabilize the interfacial monolayer (cf. Table 1 for MM-derived values). It is important to note that the MM-derived adsorption energies refer to isolated molecules in the gas phase. Desorption energies with respect to the liquid phase can be vastly different, due to stabilizing contributions from solvation enthalpy. In general, the enthalpic stabilization of monolayers at the liquid−solid interface is comprised of two major contributions, *i.e.*, from molecule−molecule interactions and from molecule−substrate interactions. When the sum of both contributions is too small to compensate the entropic cost of self-assembly, ordered structures are thermodynamically not stable at the liquid−solid interface. On the other hand, when the organic backbone becomes too large, the surface mobility can be inhibited and monolayer self-assembly can become kinetically hindered. This is obviously the

case for compounds **4** and **5** at room temperature, where only disordered adsorption occurred. Only after thermal activation does the enhanced surface mobility facilitate self-assembly of **4** into ordered structures, whereas for **5** even then the disordered structure persisted. Although the adsorption energy of **5** is lower than that of **4** and comparable to that of **3**, its surface mobility appears to be the lowest for the diboronic acids studied here. While large adsorption energies can be taken only as a hint for high surface diffusion barriers, the actual corrugation of the surface potential in relation to thermal energy determines the surface mobility. So apparently the favorable registry between the pyrene core and the graphite substrate results in strongly preferred adsorption sites that are associated with relatively deep energetic minima, hence a high corrugation of the surface potential. Disordered arrangements that are caused by a low surface mobility on graphite were even observed for comparatively small aromatic cores as in naphthalene dicarboxylic acid.[47]

Since the self-assembled monolayers emerge as an intermediate structure en route to the final 2D COF, the observed increase of the required activation temperature for polycondensation from **2** to **4** can be explained along these lines. Experimentally, we find that **2** already polymerizes below 50 °C, while **3** requires temperatures around 70 °C. For **4** even higher temperatures were necessary to observe first covalent structures. Thermal activation is needed not only to initiate the polycondensation but also to break up the preceding noncovalent arrangement, *i.e.*, the self-assembled monolayer. The enthalpic stabilization per molecule within the self-assembled monolayer increases with molecule size, thereby hinting toward a possible explanation for the increasing polymerization temperatures for monomers **2** to **4**. However, also the energetic barriers for many other processes that are vital for the thermally activated polymerization increase with monomer size. An obvious and definitely important example thereof is surface diffusion. Porte *et al*. studied the polymerization of **1** on Cu(111), Ag(100), Ag(111), and Au(111) in great detail and found the lowest degree of reticulation on Cu(111), the surface with the highest diffusion barrier.[35] Spontaneous polymerization at room temperature without further thermal activation was observed on Ag(100), yet on a time scale of tens of hours. Here the rate-determining step is most probably surface diffusion. Interestingly, polymerization starting from self-assembled monolayers of **1** on Ag(100) could be greatly accelerated either by electron bombardment or locally by STM imaging with reduced tip−sample distance.[36] The authors propose that either enhanced surface diffusion or promoted desorption could account for their observations. The poorly ordered structures observed upon room-temperature deposition of **4** and **5** clearly indicate that surface diffusion can become a limiting factor, even on weakly interacting graphite surfaces. Desorption as a competing process is another important issue for thermally activated on-surface polymerization of preceding densely packed self-assembled monolayers. For polymerization of **1** on Au(111) preferred desorption upon annealing already results in a greatly diminished surface coverage, and COFs were found only in the vicinity of substrate step-edges, where the monomers were attached more strongly. Yet, the situation at the liquid−graphite surface appears to be beneficial for polymerization as compared to metals in UHV. On one hand the surface-diffusion barriers on graphite are still quite low, and on the other hand desorption is not an irreversible process as in UHV. At the liquid−solid interface desorbing molecules are not irretrievably lost, but are still solvated in the liquid phase and available for the on-surface polymerization. Especially, when the solvent that was initially used for drop-casting evaporates during the thermal treatment, the monomer concentration in solution increases, thereby reinforcing the thermodynamic driving force for readsorption.

In summary, studying the ability of the monomer to form thermodynamically stable self-assembled structures might be useful for understanding trends in activation temperatures and the magnitudes of energetic barriers for surface diffusion and desorption.

CONCLUSION

In the present work, regular and extended 2D COFs were prepared according to a previously developed straightforward synthesis protocol.[27] Structural versatility was obtained by polycondensation of four different diboronic acids. By using para-diboronic acids where the size of the organic backbone was incrementally varied from phenyl to quaterphenyl, a series of isoreticular 2D COFs was created. The lattice parameters of these isoreticular networks range from 1.5 nm (**1**) to 3.8 nm (**4**), and the corresponding pore sizes increase from ∼1.0 to 3.2 nm. In addition, we could demonstrate that a para-diboronic acid with a pyrene core is similarly suited to yield 2D COFs with *p6mm* symmetry. For this system, indications of bilayer growth are also found with a similar eclipsed stacking to that observed in bulk crystals. In addition to their polymerization the capability of the diboronic acids to self-assemble into stable structures on the surface was studied by STM. Self-assembled, long-range ordered monolayers upon room-temperature deposition were observed only for **3**, while room-temperature deposition of **4** and **5** yielded poorly ordered structures. Since mild heating could improve the structural quality for **4** but not for **5**, a limited surface mobility at room temperature could account for the low degree of order in these kinetically trapped structures. Stable monolayers of **1** and **2** were not observed, because the

molecule–substrate interaction of these smaller molecules is too low to stabilize the interfacial monolayer.

By means of additional studies with varying activation temperature we find that for monomers **2** to **4** the temperature threshold for the onset of polymerization increases with the size of the organic backbone. Several different reaction steps, such as breaking up of hydrogen-bonded aggregates, surface diffusion, reorientation, and possibly desorption, are required to convert a noncovalent self-assembled monolayer into a surface-supported 2D COF. Since the energetic barriers of these elementary processes increase with monomer size, it is difficult to reveal the rate-determining reaction step. Hence, for a more detailed understanding of the polymerization mechanism and kinetics it would be highly desirable to study the polymerization *in situ* at the molecular scale by means of temperature-dependent STM experiments.

MATERIALS AND METHODS

The synthesis of biphenyldiboronic acid (**2**) and pyrene-2,7-diboronic acid (**5**) is reported elsewhere.[48,49] Details of the synthesis of the new diboronic acid building blocks terphenyldiboronic acid (**3**) and quaterphenyldiboronic acid (**4**) can be found in the Supporting Information. Heptanoic acid (Fluka, purity ≥98%) was used as solvent for all building blocks and additionally dodecane (Sigma-Aldrich, anhydrous, purity ≥99%) for **3**. For the 2D COF synthesis a small amount (∼1 mg) of the respective compound was added to 1.5 mL of solvent, sonicated for 90 min, and centrifuged for up to 15 min. This procedure does not fully dissolve the molecules. Subsequently, the solutions were again dispersed by careful shaking, yielding a whitish suspension. Then an amount of ∼7.5 μL of the respective suspensions was applied to a freshly cleaved (001) surface of highly oriented pyrolytic graphite (HOPG) and immediately transferred to a stainless steel reactor (7.7 mL volume) with the sample surface pointing upward. The reactor was then placed into a preheated oven for 60 min at 120 °C. Reversible reaction conditions were realized by a H_2O atmosphere that was generated by adding 50 μL of water to the bottom of the reactor (not in direct contact with the sample). A slightly opened valve on the reactor allowed gas exchange with the environment; that is, the reactor was operated as an open system. After the thermal treatment, the reactor was taken out of the oven and allowed to cool for at least 20 min before the samples were removed. After this procedure both the solvent and water were completely evaporated. Subsequently, the samples were characterized by scanning tunneling microscopy using a home-built drift-stable instrument driven by an ASC 500 scanning probe microscopy controller from attocube Systems AG. Constant current images were obtained with tunneling voltages between +0.4 and +1.1 V applied to the tip and set point currents between 40 and 110 pA. For all experiments mechanically cut 90/10 PtIr tips were used. In order to study the onset of polymerization, the influence of a thermal treatment at lower temperatures from 50 to 70 °C was studied by placing the samples directly into the oven without the reactor, thereby reducing the influence of thermal inertia.

Noncovalent self-assembly of the diboronic acid building blocks was studied directly at the liquid–solid interface. To this end, 5 μL of solution was deposited on a freshly cleaved HOPG substrate, and self-assembled monolayers were characterized with the STM tip immersed into solution.

Molecular mechanics simulations were conducted for all 2D COFs on a graphite substrate using the Dreiding force field. Similarly adsorption energies of single molecules were estimated for all building blocks. The graphite substrate was approximated by two layers with the atomic positions of the lower layer fixed. Arrangements of six unit cells were optimized for each structure.

Conflict of Interest: The authors declare no competing financial interest.

Acknowledgment. Financial support from the Nano Systems Initiative Munich (NIM) and the Bayerische Forschungsstiftung is gratefully acknowledged. D.D.M. would like to thank the Minerva Postdoctoral Fellowship.

Supporting Information Available: Synthesis of terphenyldiboronic acid (**3**) and quaterphenyldiboronic acid (**4**). This material is available free of charge *via* the Internet at http://pubs.acs.org.

REFERENCES AND NOTES

1. Perepichka, D. F.; Rosei, F. Extending Polymer Conjugation into the Second Dimension. *Science* **2009**, *323*, 216–217.
2. Joo, S. H.; Choi, S. J.; Oh, I.; Kwak, J.; Liu, Z.; Terasaki, O.; Ryoo, R. Ordered Nanoporous Arrays of Carbon Supporting High Dispersions of Platinum Nanoparticles. *Nature* **2001**, *412*, 169–172.
3. Spitler, E. L.; Dichtel, W. R. Lewis Acid-Catalysed Formation of Two-Dimensional Phthalocyanine Covalent Organic Frameworks. *Nat. Chem.* **2010**, *2*, 672–677.
4. Jiang, D. L.; Wan, S.; Guo, J.; Kim, J.; Ihee, H. A Belt-Shaped Blue Luminescent, and Semiconducting Covalent Organic Framework. *Angew. Chem., Int. Ed.* **2008**, *47*, 8826–8830.
5. Lei, S. B.; Tahara, K.; Adisoejoso, J.; Balandina, T.; Tobe, Y.; De Feyter, S. Towards Two-Dimensional Nanoporous Networks: Crystal Engineering at the Solid-Liquid Interface. *CrystEngComm* **2010**, *12*, 3369–3381.
6. Griessl, S. J. H.; Lackinger, M.; Jamitzky, F.; Markert, T.; Hietschold, M.; Heckl, W. M. Incorporation and Manipulation of Coronene in an Organic Template Structure. *Langmuir* **2004**, *20*, 9403–9407.
7. Gutzler, R.; Walch, H.; Eder, G.; Kloft, S.; Heckl, W. M.; Lackinger, M. Surface Mediated Synthesis of 2D Covalent Organic Frameworks: 1,3,5-Tris(4-bromophenyl)benzene on Graphite(001), Cu(111), and Ag(110). *Chem. Commun.* **2009**, 4456–4458.
8. Grill, L.; Dyer, M.; Lafferentz, L.; Persson, M.; Peters, M. V.; Hecht, S. Nano-Architectures by Covalent Assembly of Molecular Building Blocks. *Nat. Nanotechnol.* **2007**, *2*, 687–691.
9. Lipton-Duffin, J. A.; Ivasenko, O.; Perepichka, D. F.; Rosei, F. Synthesis of Polyphenylene Molecular Wires by Surface-Confined Polymerization. *Small* **2009**, *5*, 592–597.
10. Cai, J.; Ruffieux, P.; Jaafar, R.; Bieri, M.; Braun, T.; Blankenburg, S.; Muoth, M.; Seitsonen, A. P.; Saleh, M.; Feng, X.; *et al.* Atomically Precise Bottom-Up Fabrication of Graphene Nanoribbons. *Nature* **2010**, *466*, 470–473.
11. Lipton-Duffin, J. A.; Miwa, J. A.; Kondratenko, M.; Cicoira, F.; Sumpter, B. G.; Meunier, V.; Perepichka, D. F.; Rosei, F. Step-by-Step Growth of Epitaxially Aligned Polythiophene by Surface-Confined Reaction. *Proc. Natl. Acad. Sci. U. S. A.* **2010**, *107*, 11200–11204.
12. Blunt, M. O.; Russell, J. C.; Champness, N. R.; Beton, P. H. Templating Molecular Adsorption Using a Covalent Organic Framework. *Chem. Commun.* **2010**, *46*, 7157–7159.
13. Bieri, M.; Treier, M.; Cai, J.; Ait-Mansour, K.; Ruffieux, P.; Groning, O.; Groning, P.; Kastler, M.; Rieger, R.; Feng, X.; et al. Porous Graphenes: Two-Dimensional Polymer Synthesis with Atomic Precision. *Chem. Commun.* **2009**, *45*, 6919–6921.
14. Walch, H.; Gutzler, R.; Sirtl, T.; Eder, G.; Lackinger, M. Material- and Orientation-Dependent Reactivity for Heterogeneously Catalyzed Carbon–Bromine Bond Homolysis. *J. Phys. Chem. C* **2010**, *114*, 12604–12609.

15. Bieri, M.; Nguyen, M.-T.; Gröning, O.; Cai, J.; Treier, M.; Aït-Mansour, K.; Ruffieux, P.; Pignedoli, C. A.; Passerone, D.; Kastler; *et al*. Two-Dimensional Polymer Formation on Surfaces: Insight into the Roles of Precursor Mobility and Reactivity. *J. Am. Chem. Soc.* **2010**, *132*, 16669–16676.
16. Zwaneveld, N. A. A.; Pawlak, R.; Abel, M.; Catalin, D.; Gigmes, D.; Bertin, D.; Porte, L. Organized Formation of 2D Extended Covalent Organic Frameworks at Surfaces. *J. Am. Chem. Soc.* **2008**, *130*, 6678–6679.
17. Tanoue, R.; Higuchi, R.; Enoki, N.; Miyasato, Y.; Uemura, S.; Kimizuka, N.; Stieg, A. Z.; Gimzewski, J. K.; Kunitake, M. Thermodynamically Controlled Self-Assembly of Covalent Nanoarchitectures in Aqueous Solution. *ACS Nano* **2011**, *5*, 3923–3929.
18. Schmitz, C. H.; Ikonomov, J.; Sokolowski, M. Two-Dimensional Ordering of Poly(*p*-phenylene-terephthalamide) on the Ag(111) Surface Investigated by Scanning Tunneling Microscopy. *J. Phys. Chem. C* **2009**, *113*, 11984–11987.
19. Weigelt, S.; Busse, C.; Bombis, C.; Knudsen, M. M.; Gothelf, K. V.; Lægsgaard, E.; Besenbacher, F.; Linderoth, T. R. Surface Synthesis of 2D Branched Polymer Nanostructures. *Angew. Chem., Int. Ed.* **2008**, *47*, 4406–4410.
20. Weigelt, S.; Bombis, C.; Busse, C.; Knudsen, M. M.; Gothelf, K. V.; Lægsgaard, E.; Besenbacher, F.; Linderoth, T. R. Molecular Self-Assembly from Building Blocks Synthesized on a Surface in Ultrahigh Vacuum: Kinetic Control and Topo-Chemical Reactions. *ACS Nano* **2008**, *2*, 651–660.
21. Treier, M.; Fasel, R.; Champness, N. R.; Argent, S.; Richardson, N. V. Molecular Imaging of Polyimide Formation. *Phys. Chem. Chem. Phys.* **2009**, *11*, 1209–1214.
22. Schmitz, C. H.; Ikonomov, J.; Sokolowski, M. Two-Dimensional Polyamide Networks with a Broad Pore Size Distribution on the Ag(111) Surface. *J. Phys. Chem. C* **2011**, *115*, 7270–7278.
23. Jensen, S.; Früchtl, H.; Baddeley, C. J. Coupling of Triamines with Diisocyanates on Au(111) Leads to the Formation of Polyurea Networks. *J. Am. Chem. Soc.* **2009**, *131*, 16706–16713.
24. Faury, T.; Clair, S.; Abel, M.; Dumur, F.; Gigmes, D.; Porte, L. Sequential Linking to Control Growth of a Surface Covalent Organic Framework. *J. Phys. Chem. C* **2012**, *116*, 4819–4823.
25. Schlögl, S.; Sirtl, T.; Eichhorn, J.; Heckl, W. M.; Lackinger, M. Synthesis of Two-Dimensional Phenylene-Boroxine Networks Through in Vacuo Condensation and On-Surface Radical Addition. *Chem. Commun.* **2011**, 47.
26. Guan, C.-Z.; Wang, D.; Wan, L.-J. Construction and Repair of Highly Ordered 2D Covalent Networks by Chemical Equilibrium Regulation. *Chem. Commun.* **2012**, *48*, 2943–2945.
27. Dienstmaier, J. F.; Gigler, A. M.; Goetz, A. J.; Knochel, P.; Bein, T.; Lyapin, A.; Reichlmaier, S.; Heckl, W. M.; Lackinger, M. Synthesis of Well-Ordered COF Monolayers: Surface Growth of Nanocrystalline Precursors *versus* Direct On-Surface Polycondensation. *ACS Nano* **2011**, *5*, 9737–9745.
28. Coratger, R.; Calmettes, B.; Abel, M.; Porte, L. STM Observations of the First Polymerization Steps Between Hexahydroxy-tri-phenylene and Benzene-di-boronic Acid Molecules. *Surf. Sci.* **2011**, *605*, 831–837.
29. Sassi, M.; Oison, V.; Debierre, J. M.; Humbel, S. Modelling the Two-Dimensional Polymerization of 1,4-Benzene Diboronic Acid on a Ag Surface. *ChemPhysChem* **2009**, *10*, 2480–2485.
30. Cote, A. P.; Benin, A. I.; Ockwig, N. W.; O'Keeffe, M.; Matzger, A. J.; Yaghi, O. M. Porous, Crystalline, Covalent Organic Frameworks. *Science* **2005**, *310*, 1166–1170.
31. Stepanow, S.; Lingenfelder, M.; Dmitriev, A.; Spillmann, H.; Delvigne, E.; Lin, N.; Deng, X.; Cai, C.; Barth, J. V.; Kern, K. Steering Molecular Organization and Host-Guest Interactions Using Two-Dimensional Nanoporous Coordination Systems. *Nat. Mater.* **2004**, *3*, 229–233.
32. Spitler, E. L.; Koo, B. T.; Novotney, J. L.; Colson, J. W.; Uribe-Romo, F. J.; Gutierrez, G. D.; Clancy, P.; Dichtel, W. R. A 2D Covalent Organic Framework with 4.7-nm Pores and Insight into Its Interlayer Stacking. *J. Am. Chem. Soc.* **2011**, *133*, 19416–19421.
33. Cote, A. P.; El-Kaderi, H. M.; Furukawa, H.; Hunt, J. R.; Yaghi, O. M. Reticular Synthesis of Microporous and Mesoporous 2D Covalent Organic Frameworks. *J. Am. Chem. Soc.* **2007**, *129*, 12914–12915.
34. Wan, S.; Guo, J.; Kim, J.; Ihee, H.; Jiang, D. A Photoconductive Covalent Organic Framework: Self-Condensed Arene Cubes Composed of Eclipsed 2D Polypyrene Sheets for Photocurrent Generation. *Angew. Chem., Int. Ed.* **2009**, *121*, 5547–5550.
35. Ourdjini, O.; Pawlak, R.; Abel, M.; Clair, S.; Chen, L.; Bergeon, N.; Sassi, M.; Oison, V.; Debierre, J.-M.; Coratger, R.; *et al*. Substrate-Mediated Ordering and Defect Analysis of a Surface Covalent Organic Framework. *Phys. Rev. B* **2011**, *84*, 125421.
36. Clair, S.; Ourdjini, O.; Abel, M.; Porte, L. Tip- or Electron Beam-Induced Surface Polymerization. *Chem. Commun.* **2011**, *47*, 8028–8030.
37. Walch, H.; Maier, A.-K.; Heckl, W. M.; Lackinger, M. Isotopological Supramolecular Networks from Melamine and Fatty Acids. *J. Phys. Chem. C* **2008**, *113*, 1014–1019.
38. Tahara, K.; Furukawa, S.; Uji-i, H.; Uchino, T.; Ichikawa, T.; Zhang, J.; Mamdouh, W.; Sonoda, M.; De Schryver, F. C.; De Feyter, S.; *et al*. Two-Dimensional Porous Molecular Networks of Dehydrobenzo[12]annulene Derivatives *via* Alkyl Chain Interdigitation. *J. Am. Chem. Soc.* **2006**, *128*, 16613–16625.
39. Eddaoudi, M.; Kim, J.; Rosi, N.; Vodak, D.; Wachter, J.; O'Keeffe, M.; Yaghi, O. M. Systematic Design of Pore Size and Functionality in Isoreticular MOFs and their Application in Methane Storage. *Science* **2002**, *295*, 469–472.
40. Schlickum, U.; Decker, R.; Klappenberger, F.; Zoppellaro, G.; Klyatskaya, S.; Ruben, M.; Silanes, I.; Arnau, A.; Kern, K.; Brune; *et al.* Metal−Organic Honeycomb Nanomeshes with Tunable Cavity Size. *Nano Lett.* **2007**, *7*, 3813–3817.
41. Kuhn, P.; Antonietti, M.; Thomas, A. Porous, Covalent Triazine-Based Frameworks Prepared by Ionothermal Synthesis. *Angew. Chem., Int. Ed.* **2008**, *47*, 3450–3453.
42. Tilford, R. W.; Gemmill, W. R.; zur Loye, H. C.; Lavigne, J. J. Facile Synthesis of a Highly Crystalline, Covalently Linked Porous Boronate Network. *Chem. Mater.* **2006**, *18*, 5296–5301.
43. Langner, A.; Tait, S. L.; Lin, N.; Rajadurai, C.; Ruben, M.; Kern, K. Self-Recognition and Self-Selection in Multicomponent Supramolecular Coordination Networks on Surfaces. *Proc. Natl. Acad. Sci. U. S. A.* **2007**, *104*, 17927–17930.
44. Marschall, M.; Reichert, J.; Seufert, K.; Auwärter, W.; Klappenberger, F.; Weber-Bargioni, A.; Klyatskaya, S.; Zoppellaro, G.; Nefedov, A.; Strunskus, T.; *et al*. Supramolecular Organization and Chiral Resolution of p-Terphenyl-m-Dicarbonitrile on the Ag(111) Surface. *ChemPhysChem* **2010**, *11*, 1446–1451.
45. Rodriguez-Cuamatzi, P.; Vargas-Diaz, G.; Maris, T.; Wuest, J. D.; Hopfl, H. 1,4-Phenylenediboronic Acid. *Acta Crystallogr. E* **2004**, *60*, o1316–o1318.
46. Pawlak, R.; Nony, L.; Bocquet, F.; Olson, V.; Sassi, M.; Debierre, J. M.; Loppacher, C.; Porte, L. Supramolecular Assemblies of 1,4-Benzene Diboronic Acid on KCl(001). *J. Phys. Chem. C* **2010**, *114*, 9290–9295.
47. Heininger, C.; Kampschulte, L.; Heckl, W. M.; Lackinger, M. Distinct Differences in Self-Assembly of Aromatic Linear Dicarboxylic Acids. *Langmuir* **2008**, *25*, 968–972.
48. Coutts, I. G. C.; Goldschmid, H. R.; Musgrave, O. C. Organoboron Compounds. Part VIII. Aliphatic and Aromatic Diboronic Acids. *J. Chem. Soc. C* **1970**, 488–493.
49. Coventry, D. N.; Batsanov, A. S.; Goeta, A. E.; Howard, J. A. K.; Marder, T. B.; Perutz, R. N. Selective Ir-Catalysed Borylation of Polycyclic Aromatic Hydrocarbons: Structures of Naphthalene-2,6-bis(boronate), Pyrene-2,7-bis(boronate) and Perylene-2,5,8,11-tetra(boronate) Esters. *Chem. Commun.* **2005**, 2172–2174.